ORGANOMETALLICS

pubs.acs.org/Organometallics Article

Cationic Ru–Se Complexes for Cooperative Si–H Bond Activation

Marvin Oberling, Elisabeth Irran, Yasuhiro Ohki,* Hendrik F. T. Klare,* and Martin Oestreich*

Cite This: https://dx.doi.org/10.1021/acs.organomet.0c00719 Read Online

ACCESS | Metrics & More | Article Recommendations | Supporting Information

ABSTRACT: The preparation and structural characterization of mononuclear tethered ruthenium(II) complexes of type $[(DmpSe)Ru(PR_3)]^+BAr^F{}_4^-$ (DmpSe = 2,6-dimesitylphenyl selenolate, Ar^F = 3,5-bis(trifluoromethyl)phenyl) are described. Unlike relevant known selenolate complexes, the reported family of complexes is cationic with a single monodentate selenolate ligand. The ability of these complexes to engage in cooperative Si–H bond activation at the Ru–Se bond is investigated, and a hydrosilane adduct has been fully characterized by multinuclear NMR spectroscopy and X-ray diffraction. The usefulness of these complexes as catalysts for various ionic dehydrogenative silylation and hydrosilylation reactions is assessed. At all stages, the new complexes are compared with their thiolate homologues $[(DmpS)Ru(PR_3)]^+BAr^F{}_4^-$ (DmpS = 2,6-dimesitylphenyl thiolate). The differences between the selenolate and thiolate complexes are marginal, but measurable. The larger selenium atom provides more space around the Ru–Se bond than sulfur does for the Ru–S bond, and hence, the selenolate complexes can accommodate sterically more demanding hydrosilanes.

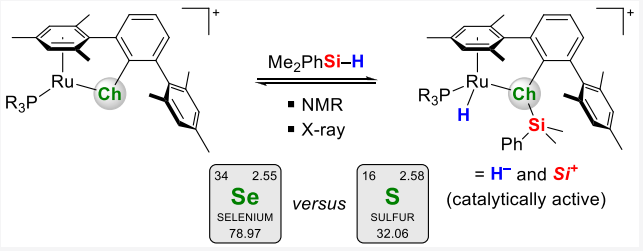

INTRODUCTION

The ability of [NiFe] hydrogenases[1] to split dihydrogen has inspired biomimetic approaches to metal thiolates[2] as novel catalysts for cooperative bond activation.[3] [NiFeSe] hydrogenases, a subclass of these enzymes with a selenocysteine residue coordinated to the nickel center instead of a cysteine, have emerged as a special point of interest, showing higher tolerance toward O_2 and enhanced H_2 production activity.[4,5] This sparked investigations employing various model complexes.[6] Despite these promising features, only a few metal selenolate complexes with catalytic application have been reported (Figure 1).[7−9] For example, Seino, Mizobe, and co-workers prepared rhodium(III) bis(selenolate) complex **1**, which was found to have a higher catalytic activity in the chemoselective hydrogenation of *N*-benzylideneaniline than the corresponding thiolate complex.[8] Also, Zhang, Luo, and co-workers recently presented nickel(II) diselenolate complex **2** and its thiolate analogue.[9a] A comparison of these two variants regarding their ability to produce H_2 revealed that the selenolate complex has a 13-times higher turnover frequency.

Our laboratories have had a long-standing interest in cooperative El–H bond activation at the Ru–S bond of cationic ruthenium(II) thiolate complexes **4** (w/ El = Si, B, Al, and Sn).[2a,c,d] These were introduced by Ohki and Tatsumi[10] and further developed in collaboration with Oestreich.[2d] The interaction of the El–H bond and the Ru–S bond generally increases the electrophilicity of the El atom and leads to heterolytic cleavage in the case of hydrosilanes.[11] The resulting sulfur-stabilized silicon electrophiles $[S–Si]^+$ together with the ruthenium hydride were broadly applicable in catalysis,[2a,d] e.g.,

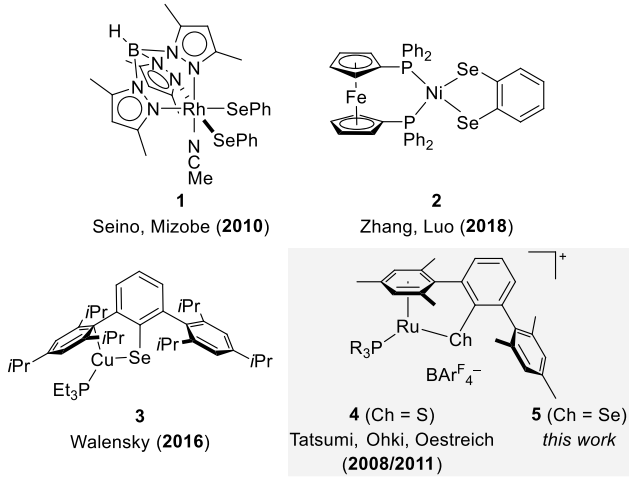

Figure 1. Selected molecular metal–selenolate complexes applied to small-molecule activation (top) and terphenyl-based complexes (bottom).

sila-Friedel–Crafts reactions,[12] pyridine hydrosilylation,[13] and dehydrogenative silylation of enolizable carbonyl com-

Received: November 10, 2020

pounds.[14] Despite these advances, we asked ourselves whether the electrophility of the silicon center could be enhanced by replacing the sulfur atom by a less Lewis-basic selenium atom. Moreover, the larger size of selenium could provide more space around the Ru−Ch bond, thereby accommodating hydrosilanes with sterically demanding substitution patterns. We describe here the synthesis of *cationic* ruthenium(II) complexes **5** containing a single Ru−Se bond. The structurally similar *neutral* copper(I) complex **3** was recently prepared by Walensky and co-workers, but their work was confined to its structural analysis.[15,16] Just as our earlier work on ruthenium(II) thiolate complexes **4**,[2d,10] the present study includes the structural characterization of a ruthenium(II) selenolate complex **5** and its hydrosilane adduct, followed by an assessment of its performance in various catalytic transformations.

RESULTS AND DISCUSSION

Synthesis and Characterization of the Cationic Ru−Se Complexes. Initially, we tried to access the selenolate complexes **5** via the established protocol for the preparation of thiolate analogues **4** by replacing the SDmp with the SeDmp ligand (Scheme 1, Route a).[10] Treatment of commercially available $[(p\text{-cymene})RuCl_2]_2$ (**6**) with LiSeDmp[17] in THF slowly resulted in a deep-blue solution, indicative of the formation of coordinatively unsaturated complex **7** (**6** → **7**). However, the subsequent reaction with Et_3P did not provide the desired complex **8a**, but led to decomposition of **7**. We therefore turned to a modified procedure in which the order of addition of the two ligands was reversed, thus avoiding a highly sensitive 16-electron intermediate (Scheme 1, Route b). As previously reported,[18] the addition of a phosphine to chloride-bridged dimer **6** gave monomeric complexes **9** (**6** → **9**), which were converted to ruthenium(II) selenolates **10** by substitution of one chloride atom with LiSeDmp (**9** → **10**). A change from CH_2Cl_2 to THF as solvent allowed performing this sequence as a one-pot process without isolating complexes **9**. Heating a solution of **10** in toluene at 95 °C led to displacement of the *p*-cymene ligand by one of the mesityl groups of the SeDmp ligand (**10** → **8**) to obtain complexes **8** as dark red powders in isolated yields of 69−78% over three steps starting from **6**. Chloride abstraction from **10** was finally achieved with 1 equiv of $NaBAr^F{}_4$, affording cationic ruthenium(II) selenolate complexes **5** as air-sensitive green solids in high yields ranging from 83% to 96% (**8** → **5**). The use of fluoro- or chlorobenzene as solvent was crucial in these reactions, since routinely used CH_2Cl_2 resulted in chloride abstraction from CH_2Cl_2 by in-situ-generated complexes **5** (for the crystallographic characterization of a Ru−Cl/$SeCH_2Cl$ adduct, see the Supporting Information).

The new cationic selenolate complexes **5** were fully characterized by multinuclear NMR spectroscopy (see Table 2 and the Supporting Information for details). The ^1H NMR spectra revealed C_s symmetry of complexes **5** in solution, as indicated by a total of four signals for the methyl groups of the SeDmp ligand. The structural assignment was further verified by successful crystallographic characterization of complex **5a**. Single crystals suitable for X-ray diffraction analysis were obtained from a solution of **5a** in a mixture of Et_2O and $(Me_3Si)_2O$ at room temperature. The solid-state structure of selenolate **5a** (Figure 2) resembles that of the thiolate congener **4a** (Table 1).[10] However, the Ru−Se bond length in **5a** is significantly longer than the Ru−S bond in **4a** (2.315 Å vs 2.212 Å),[19] as expected due to the larger size of the selenium atom compared to the sulfur atom. This is also reflected by the elongated Se−C1 bond of the SeDmp ligand in **5a** (1.936 Å vs 1.791 Å of SDmp in **4a**). Consistent with the increase of these bond lengths, the Ru−Se−C1 bond angle decreases from 101.4° for **4a** to 98.5° for **5a**. Overall, these structural parameters suggest a more exposed Ru−Se bond in **5a** compared to the Ru−S bond in **4a**, which could facilitate interaction with larger external reactants and substrates.

Scheme 1. Preparation of the Cationic Ruthenium(II) Selenolate Complexes

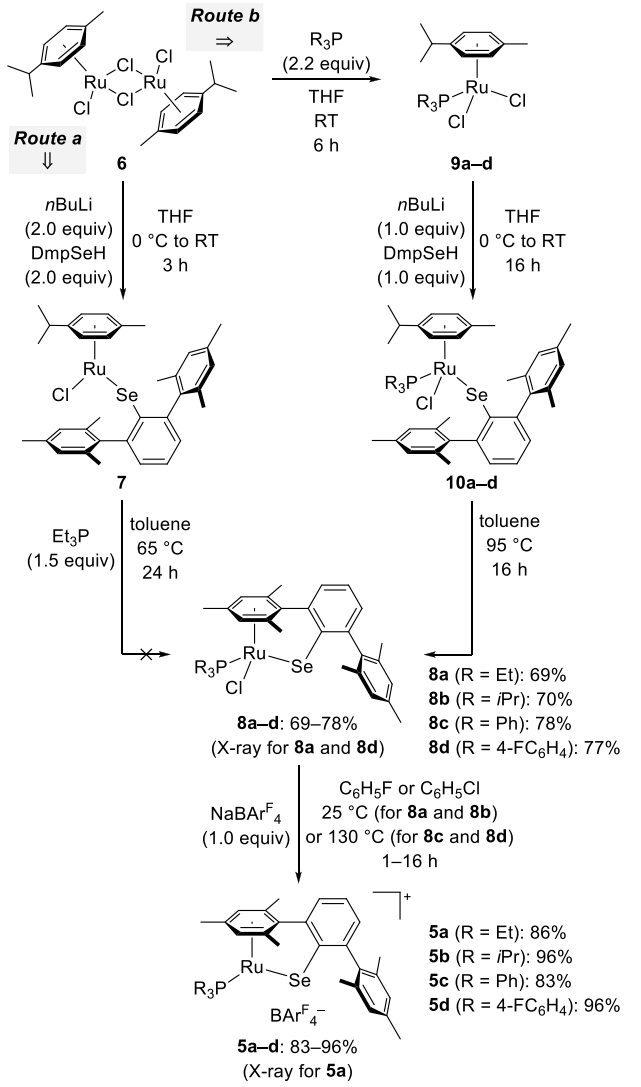

Cooperative Si−H Bond Activation at the Ru−Se Bond. To verify this hypothesis, we probed the reactivity of selenolate complexes **5a** (R_3P = Et_3P) and **5d** (R_3P = $(4\text{-}FC_6H_4)_3P$) toward hydrosilanes in the same way as we did for the corresponding thiolate complexes **4**.[11] Treatment of **5a** with 2 equiv of Me_2PhSiH (**11a**) at room temperature resulted in an immediate color change from green to yellow, indicating successful Si−H bond activation. NMR spectroscopic measurements were consistent with the formation of hydrosilane adduct **12aa** (Table 2). The ruthenium hydride was confirmed by a doublet at $\delta(^1H) = -9.06$ ppm ($^2J_{H,P} = 46.7$ Hz) in the ^1H NMR spectrum. Since chirality is (re)introduced by the additional hydride ligand, six instead of four signals are

https://dx.doi.org/10.1021/acs.organomet.0c00719
Organometallics XXXX, XXX, XXX−XXX

Table 1. Selected Bond Lengths (Å) and Angles (deg) of Thiolate 4a and Selenolate 5a (R_3P = Et_3P) and the Hydrosilane Adducts with Me_2PhSiH

	4a[a] (Ch = S)	**5a** (Ch = Se)	**4a**·Me_2PhSiH[b]	**5a**·Me_2PhSiH = **12aa**
Ru−Ch	2.2117(9)	2.3153(5)	2.3882(10)	2.4807(5)
Ch−C1	1.791(3)	1.936(4)	1.815(3)	1.975(4)
Ru−P	2.3833(10)	2.3674(14)	2.3049(10)	2.2960(12)
Ru−H			1.58(4)	1.58(4)
Ch−Si			2.2445(11)	2.3855(14)
Si···H			3.17(4)	3.38(5)
P−Ru−Ch	89.29(3)	93.06(3)	94.67(4)	92.74(3)
Ru−Ch−C1	101.38(12)	98.45(9)	102.38(12)	98.40(12)
Ru−Ch−Si			107.59(5)	106.93(4)
Si−Ch−C1			114.36(10)	111.60(15)
ΣR−Si−R			331.4	332.7

[a]Data from ref 10. [b]Data from ref 11.

Table 2. Selected NMR Spectroscopic Data of the Cooperative Si−H Bond Heterolysis of Me_2PhSiH by Selenolates 5a and 5d (Data of Thiolates 4a and 4d for Comparison)

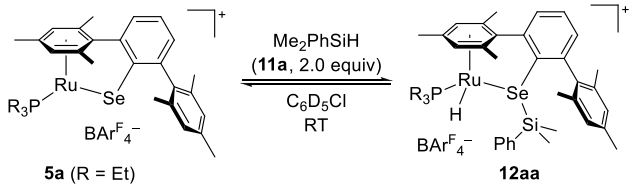

5a (R = Et)
5d (R = 4-FC_6H_4)
12aa
12da

compound	δ(^{1}H)	δ(^{29}Si)[b]	δ(^{31}P)	δ(^{77}Se)
4a[a] (Ch = S)			23.0 ppm	
4d[a] (Ch = S)			30.0 ppm	
5a (Ch = Se)			23.4 ppm	1408.5 ppm
5d (Ch = Se)			31.9 ppm	1522.5 ppm
4a·Me_2PhSiH[a]	−8.26 ppm ($^2J_{H,P}$ = 48.8 Hz)	28.4 ppm	40.4 ppm	
4d·Me_2PhSiH[a]	−7.67 ppm ($^2J_{H,P}$ = 48.5 Hz)	29.8 ppm	48.7 ppm	
5a·Me_2PhSiH = **12aa**	−9.06 ppm ($^2J_{H,P}$ = 46.7 Hz)	22.0 ppm	38.7 ppm	151.1 ppm ($^2J_{Se,P}$ = 15.3 Hz)
5d·Me_2PhSiH = **12da**	−8.27 ppm ($^2J_{H,P}$ = 47.5 Hz)	25.2 ppm	50.3 ppm	151.2 ppm ($^2J_{Se,P}$ = 31.2 Hz)

[a]Data in CD_2Cl_2 from ref 11. [b]Determined by ^{1}H/^{29}Si HMQC NMR spectroscopy.

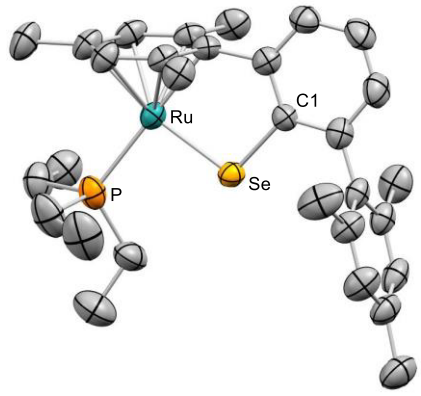

Figure 2. Molecular structure of complex **5a**. Thermal ellipsoids are shown at the 50% probability level. The counteranion and all hydrogen atoms are omitted for clarity. See Table 1 for selected bond lengths and angles.

observed for the methyl groups of the SeDmp ligand. Likewise, the *meta*-protons of the mesityl rings gave four instead of two signals. The ^{29}Si NMR chemical shift at δ(^{29}Si) = 22.0 ppm is considerably downfield-shifted relative to free Me_2PhSiH at δ(^{29}Si) = −17.3 ppm. The absence of any $^1J_{H,Si}$ satellites, which are typically observed for η^1 and η^2 hydrosilane complexes, further supported heterolytic Si−H bond cleavage and the generation of a silyl cation. Its stabilization by the selenium atom was evident in the ^{77}Se NMR spectrum, which showed a resonance at δ(^{77}Se) = 151.1 ppm ($^2J_{Se,P}$ = 15.3 Hz). The significant high-field shift compared to the precursor **5a** (δ(^{77}Se) = 1408.5 ppm) is a clear indication for an increase of the coordination number at the selenium atom due to the interaction with the positively charged silicon atom. The high-field-shifted ^{29}Si NMR chemical shift of hydrosilane adduct **12aa** compared to the corresponding thiolate congener (Δδ(^{29}Si) = 6.4 ppm) indicates a stronger interaction of the silyl cation with the selenium atom. This result is in line with studies by Müller and co-workers, who had shown for a series of intramolecular silylchalconium ions that the covalent character and stabilization of the silyl cation increases from the [S−Si]$^+$ to the [Se−Si]$^+$ linkage.[20]

The reversibility of the Si−H bond activation by selenolate complex **5a** became apparent by a ^{1}H/^{1}H NOESY NMR experiment, showing chemical exchange between the ruthenium hydride of **12aa** at δ(^{1}H) = −9.06 ppm and the hydride of free Me_2PhSiH at δ(^{1}H) = 4.55 ppm (Figure 3). In a control experiment, an equimolar mixture of Me_2PhSiH (**11a**) and deuterium-labeled Et_3SiD (**11b**-d_1) was exposed to catalytic

https://dx.doi.org/10.1021/acs.organomet.0c00719
Organometallics XXXX, XXX, XXX−XXX

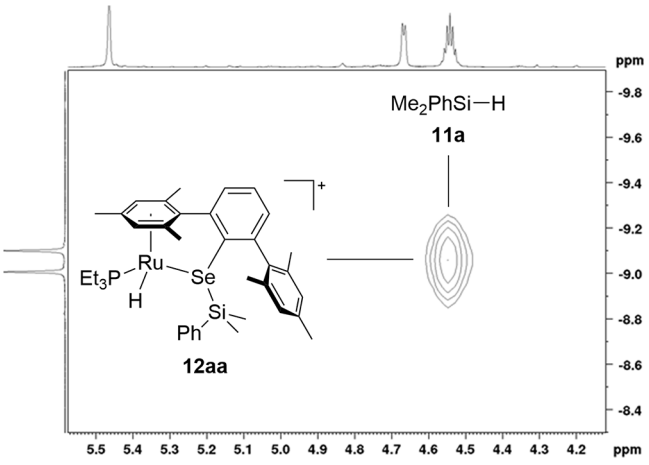

Figure 3. Selected segment of the $^{1}H/^{1}H$ NOESY NMR spectrum (500/500 MHz, C_6D_5Cl, 300 K, T_m = 600 ms) of hydrosilane adduct **12aa**.

Scheme 2. $^{1}H/^{2}H$ Scrambling Experiment

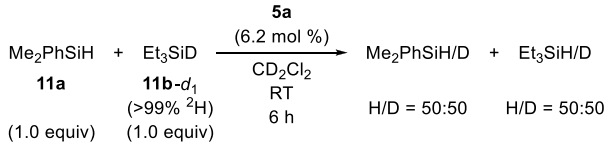

amounts of complex **5a** at room temperature, resulting in complete scrambling of the deuterium label (Scheme 2).

The molecular structure of hydrosilane adduct **12aa** was eventually determined by X-ray diffraction analysis (Figure 4).

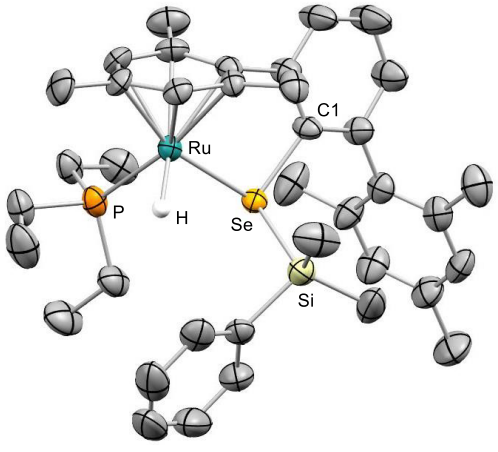

Figure 4. Molecular structure of hydrosilane adduct **12aa**. Thermal ellipsoids are shown at the 50% probability level. The counteranion and all hydrogen atoms, except for the ruthenium hydride, are omitted for clarity. See Table 1 for selected bond lengths and angles.

Single crystals were obtained from a solution of selenolate complex **5a** in neat Me_2PhSiH (**11a**) layered with *n*-hexane at −30 °C. The solid-state structure shows the same features as the corresponding thiolate analogue **4a**·Me_2PhSiH (see Table 1). The most notable changes are again the longer bond lengths of the selenium atom. The distance of 3.38 Å between the silicon atom and the ruthenium hydride proves complete cleavage of the Si−H bond. The Se−Si bond in adduct **12aa** is elongated by around 6% compared to the S−Si bond in **4a**·Me_2PhSiH (2.3855(14) Å vs 2.2445(11) Å).[21] The average C−Si−C bond angle is 110.9° and thus closer to a tetrahedral (109.5°) than a trigonal planar (120°) coordination geometry. The slightly more pronounced pyramidalization at the silicon atom than in **4a**·Me_2PhSiH (average C−Si−C bond angle of 110.5°) indicates an increased covalent character of the $[Se-Si]^+$ linkage compared to $[S-Si]^+$, which is consistent with the observed shift of the ^{29}Si NMR resonance toward higher field (*vide supra*).[20]

Changing the electronic and steric nature of the phosphine ligand in ruthenium(II) selenolates **5** had no significant influence on the Si−H bond activation event. The NMR spectroscopic analysis of complex **5d** with an electron-deficient *para*-fluorinated triarylphosphine showed the overall same trends as those of complex **5a** (cf. Table 2). The heterolysis of Me_2PhSiH also proceeded smoothly with **5b** decorated with the sterically more demanding iPr_3P ligand (see the Supporting Information for the crystallographic characterization of the hydrosilane adduct **5b**·Me_2PhSiH).

Application in Catalysis. We applied Ru−Se complex **5a** as a catalyst in various reactions involving Si−H bond activation in order to contrast its qualities against its congener Ru−S complex **4a** (both with Et_3P as ligand). For this, we chose a number of established transformations (Scheme 3): electrophilic aromatic substitution of *N*-methylated indole (**13** → **14**, top),[12] dearomative hydrosilylation of pyridine (**15** → **16**, middle),[13] and dehydrogenative silylation versus hydrosilylation of acetophenone (**17** → **18**/**19**, bottom).[14] Beginning with the electrophilic C−H silylation,[12] the results with **5a** and **4a** were essentially identical when using Me_2PhSiH (**11a**), Et_3SiH (**11b**), and $MePh_2SiH$ (**11c**). However, the reaction outcome was drastically different with sterically more hindered Ph_3SiH (**11d**). No reaction was seen with **4a** as catalyst, whereas 61% yield of the silylated indole **14d** was obtained with **5a**. Apparently, the pocket with the Ru−Se bond in complex **5a** can accommodate larger hydrosilanes than that of Ru−S complex **4a**. Moving to an even bulkier hydrosilane brought out the space limitation; *tert*-butyl-substituted $tBuMe_2SiH$ (**11e**) did not participate in the Si−H bond activation. Interestingly, in-situ-generated Ru−Se complex **5d** with electron-deficient $(4\text{-}FC_6H_4)_3P$ as the ancillary ligand afforded product **14e** in 20% yield. As expected for an S_EAr, the silylation occurred exclusively in the C3 position of the indole (as verified by NMR spectroscopy and X-ray diffraction analysis of **14d**; see the Supporting Information). A control experiment with *N*-methylindole bearing another methyl group at C3 showed showed full conversion after 48 h (not shown). With the C3 position blocked, three different indoles formed with silylation at C5 or C2 or both (see the Supporting Information for details). This result hints that the Ru−Se complex **5a** is more reactive than the Ru−S complex **4a** which was reported not to catalyze this reaction.[12]

We then turned toward the regioselective hydrosilylation of pyridine (**15**)[13] using hydrosilanes **11a**−**d**. A similar picture unfolded for this pyridine reduction compared to the above silylation of indoles. The Ru−Se complex **5a** promoted the formation of the *N*-silylated 1,4-dihydrosilanes **16a**−**d**, no matter how bulky the hydrosilane is. The majority of these reactions had not been possible with the Ru−S complex **4a**.[13a]

Another reduction catalyzed by these cationic Ru−Ch complexes is the hydrosilylation of carbonyl compounds.[14] There is a twist to this reaction because these reductions

https://dx.doi.org/10.1021/acs.organomet.0c00719
Organometallics XXXX, XXX, XXX−XXX

Scheme 3. Assessment of the Ruthenium(II) Selenolate Complexes in Representative Catalytic Reactions Involving Si−H Bond Activation

Electrophilic aromatic substitution (C–H silylation)

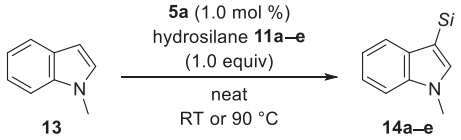

Si–H	T for t	product	yield[a]
Me_2PhSiH (**11a**)	RT for 2 h	**14a**	80% (92% w/ **4a**)[12]
Et_3SiH (**11b**)	90 °C for 48 h	**14b**	63% (67% w/ **4a**)[12]
$MePh_2SiH$ (**11c**)	RT for 6 h	**14c**	84% (88% w/ **4a**)[12]
Ph_3SiH (**11d**)	90 °C for 48 h	**14d**	61% (n.r. w/ **4a**)[12]
$tBuMe_2SiH$ (**11e**)	90 °C for 48 h	**14e**	n.r. (n.r. w/ **4a**)[12] but 20% w/ **5d**

1,4-Selective pyridine reduction

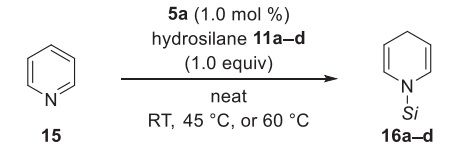

Si–H	T for t	product	yield[b]
Me_2PhSiH (**11a**)	RT for 7 h	**16a**	78% (94% w/ **4a**)[13a]
Et_3SiH (**11b**)	60 °C for 24 h	**16b**	49% (n.r. w/ **4a**)[13a]
$MePh_2SiH$ (**11c**)	45 °C for 14 h	**16c**	92% (96% w/ **4a**)[13a]
Ph_3SiH (**11d**)	60 °C for 24 h	**16d**	62% (n.r. w/ **4a**)[13a]

Dehydrogenative silylation–hydrogenation sequence

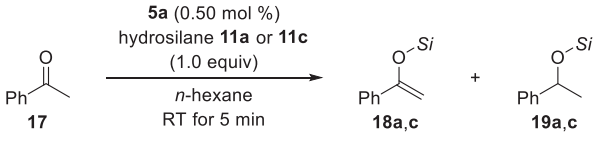

Si–H	product ratio[c]	yield[b]
Me_2PhSiH (**11a**)	**18a**:**19a** = 63:37	75%
	18a:**19a** = 85:15 (w/ **4a**)[14a]	93% (w/ **4a**)[14a]
$MePh_2SiH$ (**11c**)	**18c**:**19c** = 78:22	92%
	18c:**19c** = 83:17 (w/ **4a**)[14a]	89% (w/ **4a**)[14a]

[a]Isolated yields after purification by flash chromatography on silica gel and subsequent Kugelrohr distillation under vacuum. [b]Isolated yields after removal of the catalyst by filtration through a short plug of deactivated silica gel. [c]The chemoselectivity was determined by ^{1}H NMR spectroscopy.

mainly proceed through dehydrogenative silylation of the enolizable carbonyl compound, followed by hydrogenation of the resulting silyl enol ether with the dihydrogen released in the previous step to eventually furnish the silyl ether.[14b] Several parameters such as reaction time and closed/open vessels govern the product distribution with more silyl ether being formed at prolonged reaction times and in a closed vessel (with no escape of dihydrogen). The Lewis basicity of the chalcogen atom in the Ru−Ch complex could also become a controlling factor. The formation of the silyl enol ether traces back to α deprotonation of an intermediate silylcarboxonium ion, and this is less likely with selenium than with sulfur as the Lewis-basic site. Accordingly, the reaction of acetophenone (**17**) and Me_2PhSiH (**11a**) yielded a 63:37 mixture of silyl enol ether **18a** and silyl ether **19a** within minutes. Conversely, the same reaction catalyzed by Ru−S complex **4a** led to an 85:15 mixture, corroborating more facile α deprotonation and hence dehydrogenation.[14a] The same outcome was obtained with $MePh_2SiH$ (**11c**).

As cooperative activation of H−H at the Ru−Ch bond is also involved in the above dehydrogenation−hydrogenation reaction sequence, we also tested the hydrogenation of acetophenone (**17** → **20**, Scheme 4).[22] At 5 bar H_2 pressure,

Scheme 4. Hydrogenation of Acetophenone Catalyzed by a Ruthenium(II) Selenolate Complex

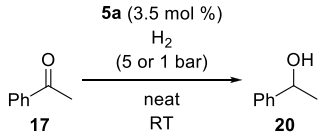

p(H2)	t	conversion[a]
5	24 h	>95% (>95% w/ **4a**)
1	48 h	76% (51% w/ **4a**)

[a]Monitored by ^{1}H NMR spectroscopy.

there was no difference between catalyst **4a** and **5a**, but we found slightly higher reactivity of Ru−Se complex **5a** at a lower H_2 pressure of 1 bar. As before, the effect is not sufficiently strong to justify a detailed comparison, but measurable.

CONCLUSION

The goal of the present study was to compare Ohki−Tatsumi ruthenium(II) thiolate complexes $[(DmpS)Ru(PR_3)]^+BAr^F{}_4^-$ with their higher homologues, the corresponding selenolate complexes $[(DmpSe)Ru(PR_3)]^+BAr^F{}_4^-$, in terms of their ability to cooperatively activate Si−H bonds and their performance as catalysts in various ionic dehydrogenative silylation and hydrosilylation reactions. The reactivity differences are in fact minor but still existent. With the selenium atom being larger than the sulfur atom, the expected finding is that the selenolate complexes can accommodate larger hydrosilanes than the thiolate complexes, e.g., Ph_3SiH. However, the catalytically generated selenium-stabilized silicon electrophile $[Se−Si]^+$ is not more reactive, i.e., electrophilic, than $[S−Si]^+$ due to more covalent character and stabilization of that linkage.[20] That stronger interaction is also seen from the ^{29}Si NMR chemical shifts of the hydrosilane adducts: high-field-shifted resonance signal for $[Se−Si]^+$ relative to $[S−Si]^+$ ($\Delta\delta(^{29}Si)$ = 4.6−6.4 ppm). There is therefore no gain in reactivity, but the new complexes expand the hydrosilane scope and are rare examples of cooperative catalysis at a metal−selenium bond.

ASSOCIATED CONTENT

Supporting Information

The Supporting Information is available free of charge at https://pubs.acs.org/doi/10.1021/acs.organomet.0c00719.

Experimental details, characterization data including NMR spectra, and crystallographic data (PDF)

Accession Codes

CCDC 2026739−2026741, 2032583−2032587, and 2039007 contain the supplementary crystallographic data for this paper. These data can be obtained free of charge via www.ccdc.cam.ac.uk/data_request/cif, or by emailing data_request@ccdc.cam.ac.uk, or by contacting The Cambridge Crystallographic Data Centre, 12 Union Road, Cambridge CB2 1EZ, UK; fax: +44 1223 336033.

AUTHOR INFORMATION

Corresponding Authors

Yasuhiro Ohki − *Department of Chemistry, Graduate School of Science, Nagoya University, Nagoya 464-8602, Japan;*

https://dx.doi.org/10.1021/acs.organomet.0c00719
Organometallics XXXX, XXX, XXX−XXX

orcid.org/0000-0001-5573-2821; Email: ohki@chem.nagoya-u.ac.jp

Hendrik F. T. Klare − *Institut für Chemie, Technische Universität Berlin, 10623 Berlin, Germany;* orcid.org/0000-0003-3748-6609; Email: hendrik.klare@tu-berlin.de

Martin Oestreich − *Institut für Chemie, Technische Universität Berlin, 10623 Berlin, Germany;* orcid.org/0000-0002-1487-9218; Email: martin.oestreich@tu-berlin.de

Authors

Marvin Oberling − *Institut für Chemie, Technische Universität Berlin, 10623 Berlin, Germany;* orcid.org/0000-0002-4917-5608

Elisabeth Irran − *Institut für Chemie, Technische Universität Berlin, 10623 Berlin, Germany;* orcid.org/0000-0001-6098-1996

Complete contact information is available at: https://pubs.acs.org/10.1021/acs.organomet.0c00719

Notes

The authors declare no competing financial interest.

■ ACKNOWLEDGMENTS

This work was supported by Grants-in-Aid for Scientific Research (19H02733 and 20K21207 for Y.O.) from the Japanese Ministry of Education, Culture, Sports, Science and Technology (MEXT), the Tatematsu Foundation, and the Yazaki Memorial Foundation. M.O. is indebted to the Einstein Foundation Berlin for an endowed professorship. We also thank Dr. Sebastian Kemper (TU Berlin) for expert advice with the NMR measurements.

■ REFERENCES

(1) Lubitz, W.; Ogata, H.; Rüdiger, O.; Reijerse, E. Hydrogenases. *Chem. Rev.* **2014**, *114*, 4081−4148.

(2) (a) Forster, F.; Oestreich, M. Metal-Ligand Cooperative Si-H Bond Activation. In *Organosilicon Chemistry: Novel Approaches and Reactions*; Hiyama, T., Oestreich, M., Eds.; Wiley-VCH: Weinheim, 2019; pp 115−130. (b) Higashi, T.; Kusumoto, S.; Nozaki, K. Cleavage of Si-H, B-H, and C-H Bonds by Metal-Ligand Cooperation. *Chem. Rev.* **2019**, *119*, 10393−10402. (c) Forster, F.; Oestreich, M. Bioinspired Catalytic Generation of Main-group Electrophiles by Cooperative Bond Activation. *Chimia* **2018**, *72*, 584−588. (d) Omann, L.; Königs, C. D. F.; Klare, H. F. T.; Oestreich, M. Cooperative Catalysis at Metal-Sulfur Bonds. *Acc. Chem. Res.* **2017**, *50*, 1258−1269.

(3) For general reviews of metal−ligand cooperation, see: (a) Khusnutdinova, J. R.; Milstein, D. Metal-Ligand Cooperation. *Angew. Chem., Int. Ed.* **2015**, *54*, 12236−12273. (b) Peters, R. *Cooperative Catalysis*; Wiley-VCH: Weinheim, 2015. (c) Grützmacher, H. Cooperating Ligands in Catalysis. *Angew. Chem., Int. Ed.* **2008**, *47*, 1814−1818.

(4) (a) Wombwell, C.; Caputo, C. A.; Reisner, E. [NiFeSe]-Hydrogenase Chemistry. *Acc. Chem. Res.* **2015**, *48*, 2858−2865. (b) Baltazar, C. S. A.; Marques, M. C.; Soares, C. M.; DeLacey, A. M.; Pereira, I. A. C.; Matias, P. M. Nickel-Iron-Selenium Hydrogenases - An Overview. *Eur. J. Inorg. Chem.* **2011**, 948−962.

(5) Reich, H. J.; Hondal, R. J. Why Nature Chose Selenium. *ACS Chem. Biol.* **2016**, *11*, 821−841.

(6) (a) Wombwell, C.; Reisner, E. Synthesis, structure and reactivity of Ni site models of [NiFeSe] hydrogenases. *Dalton Trans.* **2014**, *43*, 4483−4493. (b) Wombwell, C.; Reisner, E. Synthetic Active Site Model of the [NiFeSe] Hydrogenase. *Chem. - Eur. J.* **2015**, *21*, 8096−8104.

(7) For a review of selenium-based ligands in catalysis, see: Kumar, A.; Rao, G. K.; Saleem, F.; Singh, A. K. Organoselenium ligands in catalysis. *Dalton Trans.* **2012**, *41*, 11949−11977.

(8) Seino, H.; Misumi, Y.; Hojo, Y.; Mizobe, Y. Heterolytic H_2 activation by rhodium thiolato complexes bearing the hydrotris(pyrazolyl)borato ligand and application to catalytic hydrogenation under mild conditions. *Dalton Trans.* **2010**, *39*, 3072−3082.

(9) (a) Pan, Z.-H.; Tao, Y.-W.; He, Q.-F.; Wu, Q.-Y.; Cheng, L.-P.; Wei, Z.-H.; Wu, J.-H.; Lin, J.-Q.; Sun, D.; Zhang, Q.-C.; Tian, D.; Luo, G.-G. The Difference Se Makes: A Bio-Inspired Dppf-Supported Nickel Selenolate Complex Boosts Dihydrogen Evolution with High Oxygen Tolerance. *Chem. - Eur. J.* **2018**, *24*, 8275−8280. See also: (b) Downes, C. A.; Marinescu, S. C. Bioinspired Metal Selenolate Polymers with Tunable Mechanistic Pathways for Efficient H_2 Evolution. *ACS Catal.* **2017**, *7*, 848−854. (c) Xie, A.; Tao, Y.-W.; Peng, C.; Luo, G.-G. A nickel pyridine-selenolate complex for the photocatalytic evolution of hydrogen from aqueous solutions. *Inorg. Chem. Commun.* **2019**, *110*, 107598.

(10) Ohki, Y.; Takikawa, Y.; Sadohara, H.; Kesenheimer, C.; Engendahl, B.; Kapatina, E.; Tatsumi, K. Reactions at the Ru-S Bonds of Coordinatively Unsaturated Ruthenium Complexes with Tethered 2,6-Dimesitylphenyl Thiolate. *Chem. - Asian J.* **2008**, *3*, 1625−1635.

(11) Stahl, T.; Hrobárik, P.; Königs, C. D. F.; Ohki, Y.; Tatsumi, K.; Kemper, S.; Kaupp, M.; Klare, H. F. T.; Oestreich, M. Mechanism of the cooperative Si-H bond activation at Ru-S bonds. *Chem. Sci.* **2015**, *6*, 4324−4334.

(12) Klare, H. F. T.; Oestreich, M.; Ito, J.-I.; Nishiyama, H.; Ohki, Y.; Tatsumi, K. Cooperative Catalytic Activation of Si-H Bonds by a Polar Ru-S Bond: Regioselective Low-Temperature C-H Silylation of Indoles under Neutral Conditions by a Friedel-Crafts Mechanism. *J. Am. Chem. Soc.* **2011**, *133*, 3312−3315.

(13) (a) Königs, C. D. F.; Klare, H. F. T.; Oestreich, M. Catalytic 1,4-Selective Hydrosilylation of Pyridines and Benzannulated Congeners. *Angew. Chem., Int. Ed.* **2013**, *52*, 10076−10079. (b) Bähr, S.; Oestreich, M. A Neutral Ru^{II} Hydride Complex for the Regio- and Chemoselective Reduction of *N*-Silylpyridinium Ions. *Chem. - Eur. J.* **2018**, *24*, 5613−5622.

(14) (a) Königs, C. D. F.; Klare, H. F. T.; Ohki, Y.; Tatsumi, K.; Oestreich, M. Base-Free Dehydrogenative Coupling of Enolizable Carbonyl Compounds with Silanes. *Org. Lett.* **2012**, *14*, 2842−2845. (b) Bähr, S.; Oestreich, M. Hidden Enantioselective Hydrogenation of N-Silyl Enamines and Silyl Enol Ethers in Net C=N and C=O Hydrosilylations Catalyzed by Ru-S Complexes with One Monodentate Chiral Phosphine Ligand. *Organometallics* **2017**, *36*, 935−943.

(15) Rungthanaphatsophon, P.; Barnes, C. L.; Walensky, J. R. Copper(I) clusters with bulky dithiocarboxylate, thiolate, and selenolate ligands. *Dalton Trans.* **2016**, *45*, 14265−14276.

(16) For a neutral ruthenium(II) bis(selenolate) complex used in stoichiometric reactions, see: Ng, W.-M.; Guo, X.; Cheung, W.-M.; So, Y.-M.; Chong, M.-C.; Sung, H. H.-Y.; Williams, I. D.; Lin, Z.; Leung, W.-H. 4-Coordinated, 14-electron ruthenium(II) chalcogenolate complexes: synthesis, electronic structure and reactions with $PhICl_2$ and organic azides. *Dalton Trans.* **2019**, *48*, 13315−13325.

(17) Ellison, J. J.; Ruhlandt-Senge, K.; Hope, H. H.; Power, P. P. Synthesis and Characterization of the New Selenolate Ligand − SeC_6H_3-2,6-Mes_2 (Mes = C_6H_2-2,4,6-Me_3) and Its Two-Coordinate Zinc and Manganese Derivatives: Factors Affecting Bending in Two-Coordinate Metal Complexes with Aryl-Substituted Ligands. *Inorg. Chem.* **1995**, *34*, 49−54.

(18) Serron, S. A.; Nolan, S. P. Enthalpies of Reaction of $((p\text{-cymene})RuCl_2)_2$ with Monodentate Tertiary Phosphine Ligands. Importance of Both Steric and Electronic Ligand Factors in a Ruthenium(II) System. *Organometallics* **1995**, *14*, 4611−4616.

(19) Slightly higher Ru−Se bond lengths between 2.408 and 2.56 Å have been reported for neutral ruthenium(II) selenolate complexes: (a) Reference 16. (b) Yao, Z.-J.; Xu, B.; Su, G.; Jin, G.-X. B−H bond activation half-sandwich Ir and Ru complexes containing carboranylamidinate selenolate ligands. *J. Organomet. Chem.* **2012**, *721*−*722*, 31−35. (c) Hu, J.; Wen, J.; Wu, D.; Zhang, R.; Liu, G.; Jiang, Q.; Li,

Y.; Yan, H. Multinuclear Self-Assembly via a (*p*-Cymene)ruthenium Unit and an *o*-Carborane Selenolate Ligand. *Organometallics* **2011**, *30*, 298−304.

(20) (a) Kordts, N.; Künzler, S.; Rathjen, S.; Sieling, T.; Großekappenberg, H.; Schmidtmann, M.; Müller, T. Silyl Chalconium Ions: Synthesis, Structure and Application in Hydrodefluorination Reactions. *Chem. - Eur. J.* **2017**, *23*, 10068−10079. (b) Kunzler, S.; Rathjen, S.; Merk, A.; Schmidtmann, M.; Muller, T. An Experimental Acidity Scale for Intramolecularly Stabilized Silyl Lewis Acids. *Chem. - Eur. J.* **2019**, *25*, 15123−15130. (c) Müller, T.; Künzler, S.; Rathjen, S.; Rüger, K.; Würdemann, M. S.; Wernke, M.; Tholen, P.; Girschik, C.; Schmidtmann, M.; Landais, Y. Chiral Chalcogenyl-Substituted Naphthyl- and Acenaphthyl-Silanes and Their Cations. *Chem. - Eur. J.* 2020. DOI: 10.1002/chem.202002977. See also: (d) Marchand, C. M.; Pidun, U.; Frenking, G.; Grützmacher, H. Structure and Stability of Y-Conjugated Silylium Cations $[Si(XH)_3]^+$ (X = O, S, Se, and Te). *J. Am. Chem. Soc.* **1997**, *119*, 11078−11085.

(21) For comparison, the Se−Si bond length in neutral (terphenylseleno)silane $Trip_2C_6H_3SeSiMe_2tBu$ (Trip = 2,4,6-triisopropylphenyl) is 2.291 Å: Poleschner, H.; Ellrodt, S.; Malischewski, M.; Nakatsuji, J.-Y.; Rohner, C.; Seppelt, K. $Trip_2C_6H_3SeF$: The First Isolated Selenenyl Fluoride. *Angew. Chem., Int. Ed.* **2012**, *51*, 419−422.

(22) (a) Sakamoto, M.; Ohki, Y.; Kehr, G.; Erker, G.; Tatsumi, K. Catalytic hydrogenation of C=O and C=N bonds via heterolysis of H_2 mediated by metal-sulfur bonds of rhodium and iridium thiolate complexes. *J. Organomet. Chem.* **2009**, *694*, 2820−2824. (b) Lefranc, A.; Qu, Z.-W.; Grimme, S.; Oestreich, M. Hydrogenation and Transfer Hydrogenation Promoted by Tethered Ru-S Complexes: From Cooperative Dihydrogen Activation to Hydride Abstraction/Proton Release from Dihydrogen Surrogates. *Chem. - Eur. J.* **2016**, *22*, 10009−10016.

https://dx.doi.org/10.1021/acs.organomet.0c00719
Organometallics XXXX, XXX, XXX−XXX